

Phosphatidylethanolamine Enhances Amyloid Fiber-Dependent Membrane Fragmentation

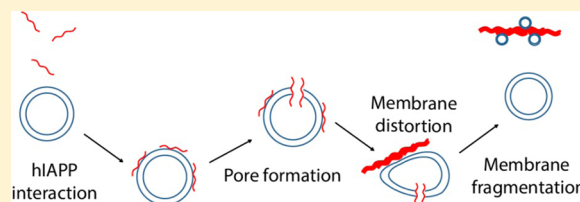
Michele F. M. Sciacca,[†] Jeffrey R. Brender,[†] Dong-Kuk Lee,^{†,‡} and Ayyalusamy Ramamoorthy^{*,†}

[†]Departments of Biophysics and Chemistry, University of Michigan, Ann Arbor, Michigan 48109-1055, United States

[‡]Department of Fine Chemistry, Seoul National University of Science and Technology, Seoul, Korea 139-743

S Supporting Information

ABSTRACT: The toxicity of amyloid-forming peptides has been hypothesized to reside in the ability of protein oligomers to interact with and disrupt the cell membrane. Much of the evidence for this hypothesis comes from in vitro experiments using model membranes. However, the accuracy of this approach depends on the ability of the model membrane to accurately mimic the cell membrane. The effect of membrane composition has been overlooked in many studies of amyloid toxicity in model systems. By combining measurements of membrane binding, membrane permeabilization, and fiber formation, we show that lipids with the phosphatidylethanolamine (PE) headgroup strongly modulate the membrane disruption induced by IAPP (islet amyloid polypeptide protein), an amyloidogenic protein involved in type II diabetes. Our results suggest that PE lipids hamper the interaction of prefibrillar IAPP with membranes but enhance the membrane disruption correlated with the growth of fibers on the membrane surface via a detergent-like mechanism. These findings provide insights into the mechanism of membrane disruption induced by IAPP, suggesting a possible role of PE and other amyloids involved in other pathologies.



The accumulation of particular proteins into long fibrillar aggregates with a characteristic β -sheet structure known as amyloids is a common feature of many devastating aging-related pathologies.^{1,2} In type II diabetes mellitus, the main constituent of these aggregates is islet amyloid polypeptide (IAPP),³ a 37-residue peptide (sequence shown in Figure 1)



Figure 1. Amino acid sequence of IAPP. IAPP is amidated in its physiologically occurring form and contains a disulfide bond between Cys2 and Cys7.

involved with insulin in glucose homeostasis.⁴ Like that of many other amyloidogenic proteins, the aggregation of IAPP has been linked to cellular dysfunction and death.⁵ Although the molecular mechanisms underlying the cytotoxicity of IAPP have not been fully elucidated, substantial evidence suggests that at least part of the toxicity of aggregates of IAPP and other amyloidogenic proteins is due to the disruption of the plasma and possibly organelle membranes during aggregation.^{6–8} The exact mechanism of membrane disruption is not yet fully understood, although several studies have proposed either the formation of transmembrane oligomeric pores,^{9–12} nonspecific ion permeation caused by binding of oligomers to the membrane surface,⁹ or a detergent-like membrane dissolution caused by the growth of amyloid fibrils on the membrane surface.^{13–15}

Most mechanistic data for IAPP-induced membrane disruption at the molecular level have come from in vitro

studies of model membranes.¹⁶ In most studies, a simplified membrane composition consisting of a single zwitterionic lipid (PC) and a single charged lipid (PG or PS) has been used.^{13,17–25} The net surface charge is an important property of the membrane that can strongly affect both the level of membrane disruption and the kinetics of amyloid formation. However, it is only one element in a large set of properties that define a realistic cell membrane mimetic. Alterations of other membrane properties have been shown to have large effects on the activity of other membrane active peptides and amyloid proteins.^{26–29} Even subtle changes in membrane composition can give rise to synergistic effects and emergent phenomena. For example, α -synuclein, an amyloidogenic protein implicated in Parkinson's disease, binds weakly to PC and PE alone but strongly to PS/PE mixed membranes.²⁷ Similarly, phase separation in ternary lipid mixtures has been shown to strongly enhance membrane binding for a variety of amyloid proteins, including IAPP.^{30,31} Although the effects of some changes in membrane composition have been studied for IAPP, the effects of many have been unexplored.^{32–34}

A particularly interesting membrane property in this context is the intrinsic curvature of the membrane, which is related to the shape of the individual lipids. The growth of amyloid fibers on the membrane can severely distort the shape of lipid vesicles, disrupting membrane integrity as the fiber becomes longer.^{14,29,35,36} The stress on the membrane induced by this

Received: July 23, 2012

Revised: September 11, 2012

Published: September 12, 2012



distortion is related to the composition of the membrane, as bending a membrane to a geometry opposed by its intrinsic curvature is an unfavorable process.³⁷ The ability of several IAPP variants to disrupt β -cell membranes is correlated with the ability to cause negative (outward) curvature in the membrane, suggesting a possible role for intrinsic lipid curvature in membrane disruption by IAPP.^{16,38} Similarly, a recent paper shows that decreasing the content of lipids with the phosphatidylethanolamine headgroup (PE), a lipid with an intrinsic negative curvature, in neuroblastoma cells reduces the toxicity of the amyloidogenic $A\beta$ peptide implicated in Alzheimer's disease.³⁹ While PE is localized primarily in the inner leaflet in cells,⁴⁰ where it would appear to be inaccessible to extracellular amyloid fibers, recent research suggests that the most damaging amyloid oligomers actually form intracellularly where they would have access to PE.^{41,42} These studies suggest that PE lipids, which are common constituents of cell membranes, could play an important role in membrane disruption by amyloidogenic peptides.

However, in vivo studies are complicated by the multiple roles lipids serve in the human body. Besides its structural role in the membrane, PE is also involved in several cellular processes that make a direct link between a toxicity decrease upon reduction of PE levels and membrane disruption difficult.⁴³ Here we explore this link by investigating the membrane disruption induced by IAPP on model membranes composed of lipids with different intrinsic curvature by adding either POPE or lysoPC, a single-chain fatty acid with the opposite curvature of PE, into vesicles containing POPC and POPS. The percentage of POPS was kept constant at 30% to maintain an identical percentage of anionic lipids in each sample. Using a combination of dye leakage, ThT fluorescence, NMR, CD, and spectrofluorimetric measurements, we observed that the presence of a PE lipid decreases the extent of membrane leakage induced by IAPP in its nonfibrillar form but significantly increases the extent of leakage caused by IAPP fibers, correlating with the impact PE has on the affinity for each species for the membrane. Results from this study shed light on the mechanism at the root of the toxic effect of IAPP toward membranes and could be useful for the investigation of the behavior of other amyloid proteins.

MATERIALS AND METHODS

Materials. Human IAPP was purchased from AnaSpec (Fremont, CA) with a purity of 97%. 1-Palmitoyl-2-oleoyl-*sn*-glycero-3-phosphocholine (POPC), 1-palmitoyl-2-oleoyl-*sn*-glycero-3-phosphoethanolamine (POPE), 1-palmitoyl-2-oleoyl-*sn*-glycero-3-phospho-L-serine sodium salt (POPS), 1-palmitoyl-2-oleoyl-*sn*-glycero-3-phospho-(1'-*rac*-glycerol) sodium salt (POPG), and 1-palmitoyl-2-hydroxy-*sn*-glycero-3-phosphocholine (LysoPC) were purchased from Avanti Polar Lipids Inc. (Alabaster, AL). 1,1,1,3,3,3-Hexafluoro-2-propanol (HFIP), L- α -phosphatidylcholine, β -(pyren-1-yl)decanoyl- γ -palmitoyl (Pyrene-PC), ferric chloride hexahydrate, and ammonium thiocyanate were purchased from Sigma-Aldrich (St. Louis, MO). 6-Carboxyfluorescein was purchased from Fluka.

Preparation of Lipid Vesicles. POPC/POPS (7:3), POPE/POPC/POPS (3:4:3), and POPC/POPS/LysoPC (6.8:3:0.2) large unilamellar vesicles (LUVs) and 6-carboxyfluorescein dye-filled LUVs were prepared using standard procedures as detailed in the Supporting Information.

Dye Leakage Assay. Membrane disruption was measured by the efflux of 6-carboxyfluorescein in a 96-well plate upon addition of IAPP, as detailed in the Supporting Information.

ThT Assay. The kinetics of amyloid formation were measured using the increase of fluorescence upon binding of the commonly used amyloid-specific dye thioflavin T (ThT) as detailed in the Supporting Information.⁴⁴ Thioflavin T experiments were performed simultaneously with the dye leakage experiments, using the same microplate and the same IAPP stock solution.

CD Experiments. Binding of prefibrillar IAPP to lipid vesicles was evaluated by CD by measuring the change in ellipticity of IAPP at 222 nm due to the conformational change from random coil to α -helix occurring upon membrane binding. DMSO could not be used to disaggregate the peptide for these experiments because of the absorbance of DMSO in the far-UV region. Instead, a 250 μ M stock solution of IAPP was made in 100 μ M HCl (pH 5) at 4 $^{\circ}$ C, a condition in which the peptide is disaggregated and stable.⁴⁵ The IAPP stock solution was then diluted to 25 μ M in 10 mM phosphate buffer with 100 mM NaF (final pH of 7.4) and then titrated with POPC/POPS and POPC/POPS/POPE LUVs.

The degree of binding to the membrane was measured by recording the ellipticity at 222 nm for 30 s for each lipid:protein ratio. K_d was then calculated from the changes in the ellipticity by the one-site binding equation: $\Delta\epsilon = [\text{lipid}] - (\Delta\epsilon_0 - \Delta\epsilon_{\infty})/K_d + [\text{lipid}] + \Delta\epsilon_0$, where $\Delta\epsilon_0$ is the ellipticity at 222 nm in the absence of lipid and $\Delta\epsilon_{\infty}$ is the ellipticity at 222 nm at a saturating lipid concentration. Spectra were collected at the initial and final points of the titration to be sure that the protein was in the random coil and α -helical conformations, respectively (Figure S1 of the Supporting Information).

NMR Experiments. ^{31}P NMR spectra were obtained from an Agilent 400 MHz solid-state NMR spectrometer using a spin-echo sequence ($90^{\circ}-\tau-180^{\circ}-\tau$, $\tau = 60 \mu\text{s}$) with 35 kHz proton decoupling, a 90° pulse duration of 5 μs , and a recycle delay of 3 s. For the ^{31}P MAS spectra, control multilamellar vesicles were prepared by hydrating 9 mg of lipid film in the appropriate molar ratio with 100 μL of 10 mM Tris buffer (pH 7.4 with 100 mM NaCl). Multilamellar vesicles containing the IAPP peptide were prepared similarly except the buffer also contained 1.178 mM IAPP (peptide:lipid molar ratio of 1%). Samples packed in a 5 mm rotor were then spun with a 4.5 kHz frequency at the magic angle; 200 transients with a recycle delay of 3 s were averaged to obtain each ^{31}P NMR spectrum. For the oriented ^{31}P NMR spectra, a sample without the peptide was first prepared using a total of 3 mg of lipid as explained elsewhere.⁴⁶ After the acquisition of the initial spectrum, 200 μL of buffer [10 mM Tris (pH 7.4) with 100 mM NaCl] containing 196 μM IAPP (peptide:lipid molar ratio of 1%) was added to the bag containing the lipid matrix, and spectra were acquired at the times indicated. All spectra were processed using 10 Hz line broadening. All experiments were performed at 37 $^{\circ}$ C, and all spectra were referenced externally to phosphoric acid (0 ppm).

Lipid Translocation Assay. Lipid translocation was measured by the ratiometric change in the fluorescence of pyrene-labeled lipids that occurs after translocation because of the dilution of the pyrene probe (Figure S2),⁴⁷ as detailed in the Supporting Information.

Membrane Fragmentation Assay. The amount of membrane fragmentation during fiber formation was quantified by measuring the lipid concentration in the supernatant after

centrifugation of 1000 nm diameter LUVs incubated with IAPP for 5 h in 10 mM phosphate buffer and 100 mM NaCl (pH 7.4). Lipid concentrations were measured colorimetrically by reaction with ammonium ferrioxalate following extraction in chloroform using a calibration curve prepared for each lipid composition.⁴⁸ Samples were spun at 14000 rpm for 40 min to pellet nonfragmented vesicles. Each experiment was performed in triplicate.

RESULTS

PE Decreases the Extent of Membrane Disruption during the Lag Phase. Membrane disruption by IAPP is a two-stage process with distinct fiber-dependent and fiber-independent phases.²⁴ Amyloid fibril formation typically follows a sigmoidal time course, with an initial lag phase reflecting the time required to build up an appreciable population of energetically unfavorable nuclei before fiber formation can begin.⁴⁹ The second phase has the characteristic sigmoidal kinetics associated with fibril growth and has been correlated with membrane damage through fiber growth on the membrane through seeding experiments and the use of amyloid inhibitors that block fiber growth.^{14,24,29,46} The origin of the first phase is less clear, but it is not dependent on fiber growth as some nonamyloidogenic analogues of IAPP show a similar effect.^{17,22,23,50} Instead, the first phase may reflect either the formation of channels or a nonspecific bilayer thinning process^{9,17,22,23,29,50} observed for some membrane-lytic antimicrobial peptides.⁵¹ Although the two-step mechanism has been reported for IAPP, evidence suggests many amyloid proteins may have similar fiber-dependent^{52–55} and fiber-independent^{56,57} phases.

To investigate how incorporating lipids with different intrinsic curvature affects each stage of IAPP-induced membrane disruption, we followed membrane disruption by a dye-release assay (Figure 2A) along with measurements of fibrillogenesis by the fiber-specific dye ThT (Figure 3) at varying peptide:lipid ratios (Figures S3 and S4 of the Supporting Information). Fiber formation was slower in the presence of both membrane types than in solution, which is typical of fiber formation at the low peptide:lipid ratios used here.^{29,58} A two-phase membrane disruption was found in all membrane types, although the kinetics and amount released in each phase differed according to the membrane composition (Figure 2A). In all samples, we observed an initial rapid increase in the fluorescence after the addition of IAPP that plateaued as time progressed (Figure 2A and Figure S3 of the Supporting Information). This initial phase of membrane disruption can be accurately modeled by a double exponential (dotted lines) and reaches a level close to the final intensity before fiber formation begins for all samples (Figures 2A and 3 and Figures S3 and S4 of the Supporting Information). The degree of membrane disruption in both phases decreases as the peptide:lipid ratio decreases, indicating membrane disruption is cooperative (Figure 2A and Figure S3 of the Supporting Information).^{17,23}

Our results suggest that PE suppresses this initial phase of membrane disruption. The degree of membrane disruption in the samples without PE (8.3%) is nearly twice that of the PE samples at the 45 min mark before the onset of fiber formation (3.6%; $p < 0.001$) (Figure 2A). In contrast to PE, the inclusion of 2% LysoPC in the vesicles had little effect on this phase of membrane disruption (Figure 2A and Figure S3 of the Supporting Information), however, LysoPC was incorporated

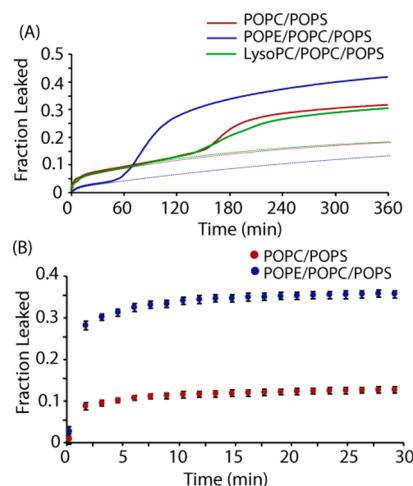


Figure 2. Membrane disruption induced by IAPP. (A) Release of 6-carboxyfluorescein from 250 μ M POPC/POPS (7:3), POPE/POPC/POPS (3:4:3), or POPC/POPS/LysoPC (6.8:3:0.2) large unilamellar vesicles (LUVs) induced by 2.5 μ M IAPP. The initial phase of membrane disruption was fitted with a double-exponential curve (dotted lines). The presence of POPE decreases the amount of dye released during the first phase and markedly increases the efficiency of dye release during the second phase. (B) Release of 6-carboxyfluorescein from seeded fibril growth. Error bars indicate the standard error of measurement. All experiments were performed in triplicate at 25 $^{\circ}$ C in 10 mM phosphate buffer and 100 mM NaCl (pH 7.4).

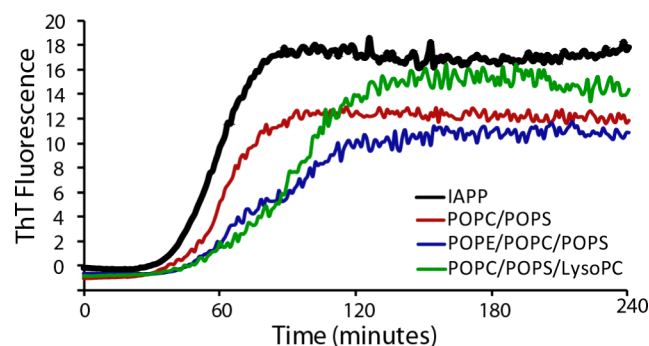


Figure 3. IAPP fiber formation kinetics measured by ThT fluorescence. Fiber formation was measured in the presence of 250 μ M POPC/POPS (7:3), POPE/POPC/POPS (3:4:3), and POPC/POPS/LysoPC (6.8:3:0.2) vesicles. Fiber formation in the absence of lipids is indicated by the black line. The IAPP concentration was 2.5 μ M for all samples. Experiments were performed at 25 $^{\circ}$ C in 10 mM phosphate buffer and 100 mM NaCl (pH 7.4). Results are the average of three experiments.

at a much lower concentration. This finding is different from what has been observed for the antimicrobial peptide magainin 2, in which even low concentrations of LysoPC (1.5%) strongly increase the degree of membrane disruption.⁵⁹

PE Enhances Membrane Disruption Associated with Fiber Formation. After the completion of the first phase, the fluorescence increases again as a second process begins to disrupt the membrane (Figure 2A).²⁴ The second phase of dye release shows the same sigmoidal kinetics as amyloid fibril formation (Figure S5 of the Supporting Information), indicating a correspondence between these two processes.¹⁴ However, the two curves do not coincide, as might be expected if fiber formation is directly linked to the second phase (Figures S6 and S7 of the Supporting Information).^{12,14} In fact, the

second phase occurs well after the ThT assay seems to indicate that fiber formation is essentially complete. However, the time difference between the two curves may stem from the differing sensitivities of each method. While the ThT assay measures fiber formation from all sources, the kinetics of the second phase of dye release are determined solely by the rate of fiber formation on the membrane. We therefore directly tested the influence of PE on membrane disruption by fibril growth by repeating the dye leakage experiment using preformed amyloid fibers to immediately seed amyloid growth.¹⁴ Preformed amyloid fibers by themselves did not cause membrane disruption (Figure S8 of the Supporting Information), in agreement with previous reports.^{14,60} However, the addition of a monomeric peptide to the preformed fibers caused an immediate increase in fluorescence, much larger for the sample with PE (35.9%) than that caused by monomeric IAPP alone (2.8% after 30 min) (Figure 2). The fraction of dye that leaked from samples with PE (35.9%) is roughly 3 times the amount observed from those without PE (12.7%; $p < 0.001$). This result confirms PE strongly enhances membrane disruption by fiber growth on the membrane.

Prefibrillar IAPP Binds Less Favorably to PE-Containing Membranes. The dye-release assay results suggest that the presence of PE either alters the membrane binding affinity or alters the physical properties of the membrane to make it more or less susceptible to membrane disruption by different oligomeric states of the peptide. To investigate the first of these possibilities, we evaluated PE's effect on the membrane binding affinity by performing CD (circular dichroism) experiments and measuring the conformational change in IAPP from a random coil to α -helix that initially occurs upon binding to the membrane.²⁵ We followed this conformational transition by titrating a 25 μ M solution of IAPP with a solution of vesicles and recording the ellipticity at 222 nm. Our results show that PE reduces the binding affinity of prefibrillar IAPP for the membrane (Figure 4; $K_d = 190 \pm 85 \mu$ M for PC/PS LUVs, and $K_d = 790 \pm 270 \mu$ M for PE/PC/PS LUVs), consistent with the observation that the initial phase of dye release during the lag phase is shorter in the presence of PE (Figure 2). However, the amount of dye released in the fiber-dependent second phase is

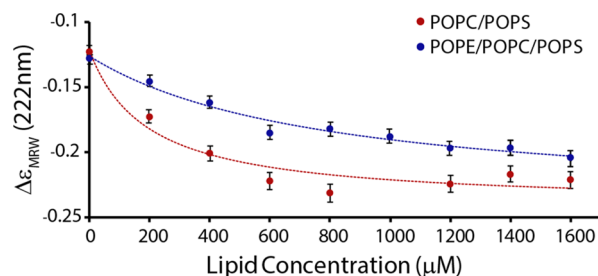


Figure 4. Binding of prefibrillar IAPP to lipid vesicles. Changes in molar ellipticity at 222 nm arising from the coil-to-helix conformational change upon membrane binding as a function of lipid concentration. Freshly dissolved IAPP (25 μ M) was titrated with the indicated concentrations of 7:3 POPC/POPS (●) and 3:4:3 POPE/POPC/POPS (○) LUVs. The final conformation of IAPP is similar in both membranes (Figure S1 of the Supporting Information). Lines represent binding isotherms to each data set. Experiments were performed at 25 °C in 10 mM phosphate buffer and 100 mM NaF (pH 7.4). Measurements represent the average of 30 measurements over 30 s, and error bars indicate the standard deviation of this measurement.

significantly higher in the presence of PE, suggesting either PE binds the amyloid fiber more tightly than prefibrillar IAPP or membranes containing PE are particularly susceptible to fiber-catalyzed membrane disruption.

IAPP Amyloid Fibers Interact More Strongly with PE Than PC in Mixed Membranes. The CD analysis described above relies on the conformational change from the random coil to α -helical state that occurs when prefibrillar IAPP binds to the lipid bilayer. Because amyloid fibers remain in the β -sheet conformation when bound to the membrane, such an analysis cannot determine the interactions of the amyloid fiber with the membrane. Instead, ³¹P solid-state NMR experiments were employed to directly measure the perturbation of each lipid component occurring when IAPP was added at a high concentration to mixed bilayers (Figure 5). POPC and POPS

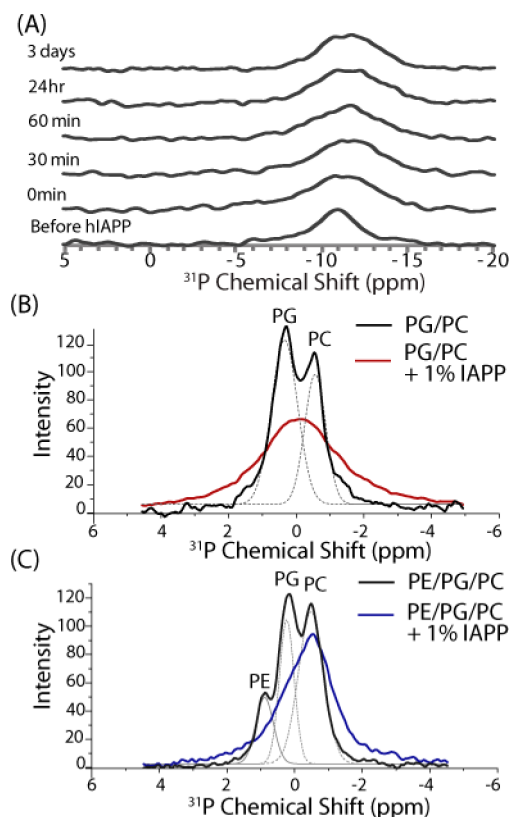


Figure 5. ³¹P NMR spectra revealing the interaction of IAPP amyloid fibers with lipid vesicles. (A) Time-dependent static ³¹P NMR spectra of aligned bilayers after the addition of 1 mol % IAPP. Changes are not apparent in subsequent spectra after the addition of IAPP, suggesting IAPP reached the amyloid state before the first spectrum was acquired. (B and C) Magic angle spinning ³¹P NMR spectra of (B) 7:3 POPC/POPG and (C) 3:4:3 POPE/POPG/POPC multilamellar vesicles incubated with 1.178 mM (1 mol %) IAPP. Dotted lines represent a deconvolution of the spectrum. Experiments were performed at 37 °C in 10 mM Tris buffer and 100 mM NaCl (pH 7.4).

have very similar ³¹P chemical shifts and cannot be resolved even by two-dimensional NMR techniques.⁶¹ For this reason, POPG was substituted for POPS in the ³¹P NMR experiment, as they have the same charge and similar intrinsic curvature. Successive scans of aligned PC/PG/PE bilayers incubated with IAPP did not change significantly with incubation time (Figure 5A), suggesting amyloid formation is rapid at the high peptide concentrations used and confirming the changes seen in Figure

5 are reflective of the interaction of amyloid fibers with the bilayer.

In the absence of IAPP, the resonances are reasonably well resolved under magic angle spinning to identify the individual components of the bilayer (dotted lines, Figure 5B,C). The addition of IAPP substantially broadens both the PC and PG resonances in the sample without PE (Figure 5B) without a noticeable change in chemical shift, most likely reflecting shorter spin–spin relaxation times due to the motional restriction of the lipid headgroup upon peptide binding.⁶² The broadening is roughly equal for PC and PG resonances, suggesting either the membrane is not phase separated or IAPP affects both lipids similarly.

The addition of PE to the membrane has a substantial effect on the broadening induced by IAPP binding. Like the membranes without PE, IAPP binding also causes broadening of the ³¹P resonances of PE-containing membranes (Figure 5C). However, unlike the membranes without PE, the broadening is not equal for all lipids. IAPP binding causes significant broadening of the PG and PE resonances, suggesting a strong interaction with the headgroup of these lipids (Figure 5C). By contrast, the resonance from PC was relatively unaffected (Figure 5C). While it is difficult to quantitate the degree of binding only from the ³¹P spectrum, the absence of significant broadening of the PC resonance indicates IAPP amyloid fibers have a weaker interaction with PC than either PG or PE in mixed membranes.

PE Enhances Detergent-like Membrane Fragmentation by IAPP. The dye-release assay does not distinguish between membrane permeabilization through the formation of specific pores or by a detergent-like mechanism. Detergent-like membrane permeabilization is characterized by the fragmentation of the membrane into small micelle- or vesicle-like structures and can be evaluated by first sedimenting large unilamellar vesicles in the presence of IAPP and then measuring lipid concentrations in the supernatant by the Stewart assay.⁴⁸ We measured the lipid concentration of the supernatant before and 5 h after the addition of IAPP (Figure 6; concentration dependence shown in Figure S9 of the Supporting Information), as previous results suggested membrane fragmentation is related to amyloidogenesis.⁴⁶ In the absence of IAPP, only a small percentage of the total lipid

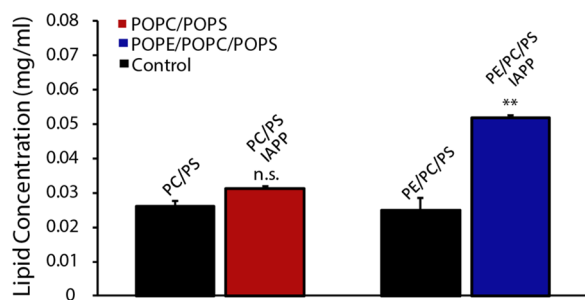


Figure 6. Membrane fragmentation induced by IAPP. IAPP (15 μ M) was incubated with 1 mg/mL large unilamellar vesicles before fragmented membranes were separated by centrifugation at 14000 rpm. Lipid concentrations were measured by the Stewart assay. All experiments were performed in 10 mM phosphate buffer and 100 mM NaCl (pH 7.4). Results are the average of three experiments, and error bars indicate the standard error of measurement. The extent of fragmentation of membranes containing PE is significantly higher than the extent of those without.

concentration was in the supernatant, confirming that almost all of the lipids had sedimented after centrifugation. Five hours after the addition of IAPP, when fiber formation is expected to be complete, significantly more lipids were found in the supernatant of the PE samples, although the amount still represented a small fraction of the total lipid. In membranes without PE, the addition of IAPP only slightly elevated the soluble fraction of the lipid (Figure 6 and Figure S9 of the Supporting Information). This finding confirms that vesicles containing PE are more prone to membrane fragmentation as the fibers form on the surface, consistent with a higher degree of dye release found in PE-containing vesicles in the fiber-dependent membrane permeabilization phase and the high affinity of the IAPP fiber for PE measured by NMR.

Fiber-Dependent Membrane Disruption by IAPP Occurs by a Detergent-like Mechanism Involving a Loss of Membrane Asymmetry. The low time resolution of the centrifugation assay and the small amount of micellelike lipids detected made its application to the initial phase of membrane disruption problematic. To test for solubilization of the membrane in this initial phase, we measured membrane fragmentation indirectly by tracking the loss of lipid bilayer asymmetry as a function of time, as it is expected that the formation of a micellelike lipid aggregate or a toroidal pore will cause significant mixing of the two leaflets of a bilayer, while a traditional barrel-stave-type pore will not.⁶³ Accordingly, we tracked lipid translocation during the first phase of membrane disruption immediately after addition of peptide using a lipid labeled with a pyrene moiety (Pyrene-PC) according to the method described by Müller et al.⁴⁷ The spectrum of pyrene is concentration-dependent, with the intensity ratio between the excimer and the monomer signal (I_E/I_M) decreasing with the pyrene concentration in an individual leaflet. When Pyrene-PC is added asymmetrically to the outer leaflet of a vesicle, a loss of bilayer asymmetry will reduce the effective pyrene concentration in the bilayer and therefore reduce the I_E/I_M ratio.

Lipid translocation was not detected in either sample (PC/PS or PE/PC/PS) within the first 30 min after the addition of freshly dissolved peptide, in contrast to the positive control MSI-78, an antimicrobial peptide that is known to cause loss of lipid asymmetry at low concentrations through the formation of a toroidal-type pore (Figure 7).⁶⁴ Because a significant amount of dye leakage occurs within this time frame under similar conditions (see Figure 2A), it is reasonable to conclude that the first phase of membrane disruption does not involve the loss of lipid asymmetry.

The evaluation of lipid translocation in the fiber-dependent second phase was hampered by the level of flip-flop occurring in the absence of peptide during prolonged observation. To solve this problem, we repeated the lipid translocation assay by first incubating the LUV sample with 1 μ M preformed hIAPP fibers before the addition of monomeric IAPP. Fiber elongation occurs immediately in the presence of preformed fibers,¹⁴ allowing observation without interference from the natural rate of flip-flop. For these samples, lipid translocation was detected immediately after the addition of monomeric IAPP (Figure 7). Translocation is more evident for samples containing PE (Figure 7B), confirming the results obtained with the lipid sedimentation and dye-release assays. This result suggests fiber-dependent membrane disruption is enhanced by the presence of PE lipids and occurs through a detergent-like mechanism, while fiber-independent membrane disruption does not involve the fragmentation of the membrane.

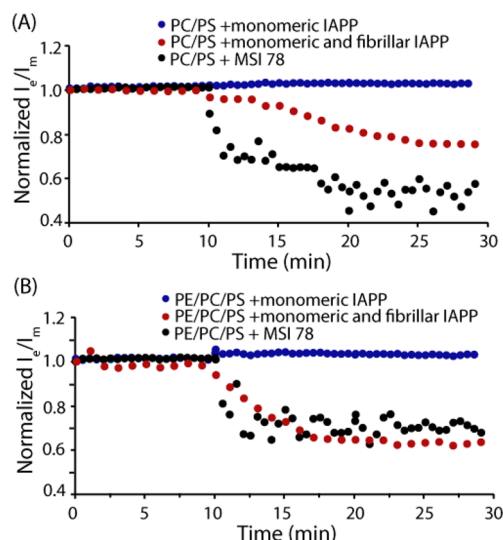


Figure 7. Loss of membrane asymmetry induced by IAPP measured by the Pyrene-PC assay. Lipid translocation induced by 1 μ M monomeric IAPP, 1 μ M monomeric IAPP in the presence of 1 μ M preformed IAPP fibers, and 0.5 μ M MSI-78 in 20 μ M (A) 7:3 POPC/POPS or (B) 3:4:3 POPE/POPC/POPS large unilamellar vesicles labeled with 3% Pyrene-PC in the outer leaflet. Both peptides were added at the 10 min mark. All experiments were performed at 37 $^{\circ}$ C in 10 mM phosphate buffer and 100 mM NaCl (pH 7.4).

DISCUSSION

Although the exact mechanism by which IAPP disrupts membranes is disputed, current evidence suggests that it has both a fiber-independent first phase and a fiber-dependent second phase. Depending on the concentration, either phase is sufficient to induce toxicity.^{23,50} Dye leakage experiments show that while PE initially suppresses the membrane disruption in the first phase, it results in a greater level of membrane fragmentation during fiber formation (Figure 2). The origins of this behavior correlate with the relative affinities of different oligomeric species of IAPP for PE. While prefibrillar IAPP has a weaker affinity for membranes containing PE (Figure 4), solid-state NMR shows that amyloid fibers of IAPP interact strongly and specifically with PE in mixed bilayers (Figure 5C). The strong interaction of amyloid fibers with PE during fiber formation is linked to a greater amount of membrane disruption by a detergent-like mechanism and the appearance of small micelle-like protein–lipid aggregates (Figure 6). This mechanism was not observed during the first phase of dye release, suggesting that the initial mechanism of disruption of the membrane does not involve the formation of micellelike structures or toroidal-type pores (Figure 7).

From these experiments, it is apparent that the membrane composition modulates the relative affinity of different conformations of IAPP for the membrane, which in turn affects the degree of membrane permeabilization in each stage of membrane disruption. Why do the two conformations of IAPP show such a difference in binding to PE? For the membrane to remain in a stable flat lamellar phase, the relative cross-sectional area of the lipid headgroup and acyl chain regions of the bilayer must be similar.³⁷ PC is easily incorporated into flat lipid bilayers, as the cylindrical shape of the molecule ensures that the lipid molecules can be tightly packed against each other without a distortion of the bilayer shape. Phosphatidylethanolamine (PE), on the other hand, is

wedge-shaped with a small headgroup compared to those of most other lipids (~ 40 \AA^2 compared to ~ 80 \AA^2 for PC).⁶⁵ The small headgroup of PE cannot be packed easily against other lipid headgroups in a lipid bilayer, which creates a stress in the membrane. This stress can be relieved by binding of peptides or proteins to the surface to the membrane, because a shallow insertion of the peptide into the bilayer can eliminate the void volume resulting from the smaller size of the PE headgroup.⁶⁵ A deeper insertion of the peptide is more unfavorable for PE than PC, as deep insertion creates additional curvature strain from the expansion of the hydrophobic core at the center of the membrane. From these considerations, we expect the inclusion of PE in the membrane should favor the binding of conformations of IAPP that bind near the membrane surface and disfavor those that insert into the hydrophobic core. LysoPC, which possesses the opposite curvature of PE, should favor the opposite localization, although it is difficult to incorporate large amounts of LysoPC into the membrane without affecting the structural integrity of the membranes.⁵⁹

The relative binding affinities of the IAPP monomer and fiber follow this pattern. Freshly dissolved IAPP, which is largely monomeric, binds more tightly to pure PC membranes (see Figure 4), as would be expected if the monomer of IAPP penetrated relatively deeply into the membrane. The position of the α -helical monomer of IAPP in the membrane is known with some certainty from EPR studies, which indicate the monomer binds parallel to the membrane surface.⁵⁸ The center of the helix (~ 6 \AA in diameter) is positioned 6–9 \AA below the phosphate group in POPS vesicles.⁵⁸ At this level, the top of the helix is in the interfacial region, 3–6 \AA below the phosphate group, and the bottom of the helix extends significantly into the hydrophobic core.⁵⁸ This finding is supported by NMR studies that show that the peptide is significantly protected from the water-soluble paramagnetic Mn^{2+} ions, which suggests a deep insertion of the peptide.⁶⁶ Interestingly, the depth of insertion appears to be related to the ability to cause membrane disruption. When H18 is protonated or mutated to Arg, the peptide binds closer to the surface and loses most of its ability to disrupt membranes and cytotoxicity.²³ Similarly, the amyloidogenic PAP_{248–286} peptide, which does not penetrate into membranes,⁶⁷ also does not cause membrane disruption or cytotoxicity.^{68,69}

While IAPP initially binds the membrane as an α -helix,^{17,25,70} it is possible that the actual pores are formed from a minority of the peptide that is in the β -sheet or another conformation. In particular, pores formed from transmembrane β -hairpins have been proposed as a model for the channels formed by A β and other amyloidogenic proteins.⁷¹ In this case, the influence of PE is likely to be indirect, as the lipid headgroup will likely have less influence on a transmembrane peptide. Because IAPP oligomers likely form on the membrane,^{45,72} PE lipids can indirectly favor the formation of such transmembrane oligomers by increasing the amount of membrane-bound IAPP.

In comparison to the IAPP monomer, few direct measurements of the positioning of amyloid fibers within the membrane have been made. However, deep insertion of amyloid fibers is virtually precluded by the substantial void volume created beneath the fiber upon insertion into the membrane. In the smaller monomeric peptide, the unfavorable increase in entropy caused by the creation of the void volume can be partially alleviated by the splaying of the lipid tails into the void volume. However, lipid splaying is less effective for amyloid fibers as the lipid tails cannot splay beneath the entire width of the fiber

because of its large size. Consistent with this, indirect measurements consistently show that amyloid fibers localize at the surface and do not penetrate deeply into the membrane.^{73,74} Because these properties are generally true of all amyloid fibers, it is likely that the binding of most, if not all, amyloid fibers to the membrane is enhanced as the PE content of the membrane is increased. It is expected, therefore, that PE and other lipids with negative curvature (such as cardiolipid) will enhance fiber-dependent membrane damage for most, if not all, amyloidogenic proteins.

■ ASSOCIATED CONTENT

■ Supporting Information

Procedures for LUV preparation, the dye-leakage assays, and the ThT and lipid translocation assays, CD spectra of IAPP in the absence and presence of membranes, pyrene emission spectra from LUVs labeled symmetrically and asymmetrically with Pyrene-PC, the effect of lipid concentration on the membrane disruption induced by IAPP and on the kinetics of IAPP fiber formation, and the concentration dependence of IAPP on membrane fragmentation. This material is available free of charge via the Internet at <http://pubs.acs.org>.

■ AUTHOR INFORMATION

Corresponding Author

*E-mail: ramamoorthy@umich.edu. Phone: (734) 647-6572.

Funding

This research was supported by funds from the National Institutes of Health (GM095640 to A.R.). D.-K.L. was supported by the Basic Science Research Program through the National Research Foundation of Korea (NRF) funded by the Ministry of Education, Science and Technology (2009-0087836).

Notes

The authors declare no competing financial interest.

■ ABBREVIATIONS

PE, phosphatidylethanolamine; IAPP, islet amyloid polypeptide; PC, phosphatidylcholine; PG, phosphatidylglycerol; PS, phosphatidylserine; NMR, nuclear magnetic resonance; CD, circular dichroism; POPC, 1-palmitoyl-2-oleoyl-*sn*-glycero-3-phosphocholine; POPE, 1-palmitoyl-2-oleoyl-*sn*-glycero-3-phosphoethanolamine; POPS, 1-palmitoyl-2-oleoyl-*sn*-glycero-3-phospho-L-serine sodium salt; POPG, 1-palmitoyl-2-oleoyl-*sn*-glycero-3-phospho-(1'-*rac*-glycerol) sodium salt; LysoPC, 1-palmitoyl-2-hydroxy-*sn*-glycero-3-phosphocholine; HFIP, 1,1,1,3,3,3-hexafluoro-2-propanol; Pyrene-PC, β -(pyren-1-yl)-decanoyl- γ -palmitoyl; ThT, thioflavin T; LUVs, large unilamellar vesicles.

■ REFERENCES

- (1) Carrell, R. W., and Lomas, D. A. (1997) Conformational disease. *Lancet* 350, 134–138.
- (2) Chiti, F., and Dobson, C. M. (2006) Protein misfolding, functional amyloid, and human disease. *Annu. Rev. Biochem.* 75, 333–366.
- (3) Westermark, P., Wernstedt, C., Wilander, E., Hayden, D. W., O'Brien, T. D., and Johnson, K. H. (1987) Amyloid fibrils in human insulinoma and islets of Langerhans of the diabetic cat are derived from a neuropeptide-like protein also present in normal islet cells. *Proc. Natl. Acad. Sci. U.S.A.* 84, 3881–3885.

- (4) Woods, S. C., Lutz, T. A., Geary, N., and Langhans, W. (2006) Pancreatic signals controlling food intake; insulin, glucagon and amylin. *Philos. Trans. R. Soc. London, Ser. B* 361, 1219–1235.
- (5) Westermark, P., Andersson, A., and Westermark, G. T. (2011) Islet amyloid polypeptide, islet amyloid, and diabetes mellitus. *Physiol. Rev.* 91, 795–826.
- (6) Kaye, R., Sokolov, Y., Edmonds, B., McIntire, T. M., Milton, S. C., Hall, J. E., and Glabe, C. G. (2004) Permeabilization of lipid bilayers is a common conformation-dependent activity of soluble amyloid oligomers in protein misfolding diseases. *J. Biol. Chem.* 279, 46363–46366.
- (7) Haataja, L., Gurlo, T., Huang, C. J., and Butler, P. C. (2008) Islet amyloid in type 2 diabetes, and the toxic oligomer hypothesis. *Endocr. Rev.* 29, 302–316.
- (8) Hebda, J. A., and Miranker, A. D. (2009) The interplay of catalysis and toxicity by amyloid intermediates on lipid bilayers: Insights from type II diabetes. *Annu. Rev. Biophys. Biomol. Struct.* 38, 125–152.
- (9) Last, N. B., Rhoades, E., and Miranker, A. D. (2011) Islet amyloid polypeptide demonstrates a persistent capacity to disrupt membrane integrity. *Proc. Natl. Acad. Sci. U.S.A.* 108, 9460–9465.
- (10) Lashuel, H. A., and Lansbury, P. T. (2006) Are amyloid diseases caused by protein aggregates that mimic bacterial pore-forming toxins? *Q. Rev. Biophys.* 39, 167–201.
- (11) Anguiano, M., Nowak, R. J., and Lansbury, P. T. (2002) Protofibrillar islet amyloid polypeptide permeabilizes synthetic vesicles by a pore-like mechanism that may be relevant to type II diabetes. *Biochemistry* 41, 11338–11343.
- (12) La Rosa, C., Scalisi, S., Sciacca, M. F. M., Zhavnerko, G., Grasso, D. M., and Marletta, G. (2010) Self-assembling pathway of hIAPP fibrils within lipid bilayers. *ChemBioChem* 11, 1856–1859.
- (13) Sparr, E., Engel, M. F. M., Sakharov, D. V., Sprong, M., Jacobs, J., de Kruijff, B., Hoppener, J. W. M., and Killian, J. A. (2004) Islet amyloid polypeptide-induced membrane leakage involves uptake of lipids by forming amyloid fibers. *FEBS Lett.* 577, 117–120.
- (14) Engel, M. F., Khemtchourian, L., Kleijer, C. C., Meeldijk, H. J., Jacobs, J., Verkleij, A. J., de Kruijff, B., Killian, J. A., and Hoppener, J. W. (2008) Membrane damage by human islet amyloid polypeptide through fibril growth at the membrane. *Proc. Natl. Acad. Sci. U.S.A.* 105, 6033–6038.
- (15) Green, J. D., Kreplak, L., Goldsberry, C., Blatter, X. L., Stolz, M., Cooper, G. S., Seelig, A., Kist-Ler, J., and Aebi, U. (2004) Atomic force microscopy reveals defects within mica supported lipid bilayers induced by the amyloidogenic human amylin peptide. *J. Mol. Biol.* 342, 877–887.
- (16) Brender, J. R., Salamekh, S., and Ramamoorthy, A. (2012) Membrane disruption and early events in the aggregation of the diabetes related peptide IAPP from a molecular perspective. *Acc. Chem. Res.* 45, 454–462.
- (17) Knight, J. D., Hebda, J. A., and Miranker, A. D. (2006) Conserved and cooperative assembly of membrane-bound α -helical states of islet amyloid polypeptide. *Biochemistry* 45, 9496–9508.
- (18) Knight, J. D., and Miranker, A. D. (2004) Phospholipid catalysis of diabetic amyloid assembly. *J. Mol. Biol.* 341, 1175–1187.
- (19) Evers, F., Jeworrek, C., Tiemeyer, S., Weise, K., Sellin, D., Paulus, M., Struth, B., Tolan, M., and Winter, R. (2009) Elucidating the mechanism of lipid membrane-induced IAPP fibrillogenesis and its inhibition by the red wine compound resveratrol: A synchrotron X-ray reflectivity study. *J. Am. Chem. Soc.* 131, 9516–9521.
- (20) Sellin, D., Yan, L. M., Kapurniotu, A., and Winter, R. (2010) Suppression of IAPP fibrillation at anionic lipid membranes via IAPP-derived amyloid inhibitors and insulin. *Biophys. Chem.* 150, 73–79.
- (21) Engel, M. F. M., Yigittop, H., Elgersma, R. C., Rijkers, D. T. S., Liskamp, R. M. J., de Kruijff, B., Hoppener, J. W. M., and Killian, J. A. (2006) Islet amyloid polypeptide inserts into phospholipid monolayers as monomer. *J. Mol. Biol.* 356, 783–789.
- (22) Brender, J. R., Lee, E. L., Cavitt, M. A., Gafni, A., Steel, D. G., and Ramamoorthy, A. (2008) Amyloid fiber formation and membrane disruption are separate processes localized in two distinct regions of

IAPP, the type-2-diabetes-related peptide. *J. Am. Chem. Soc.* 130, 6424–6429.

(23) Brender, J. R., Hartman, K., Reid, K. R., Kennedy, R. T., and Ramamoorthy, A. (2008) A single mutation in the nonamyloidogenic region of islet amyloid polypeptide greatly reduces toxicity. *Biochemistry* 47, 12680–12688.

(24) Brender, J. R., Lee, E. L., Hartman, K., Wong, P. T., Ramamoorthy, A., Steel, D. G., and Gafni, A. (2011) Biphasic effects of insulin on islet amyloid polypeptide membrane disruption. *Biophys. J.* 100, 685–692.

(25) Jayasinghe, S. A., and Langen, R. (2005) Lipid membranes modulate the structure of islet amyloid polypeptide. *Biochemistry* 44, 12113–12119.

(26) Grudzielanek, S., Smirnovas, V., and Winter, R. (2007) The effects of various membrane physical-chemical properties on the aggregation kinetics of insulin. *Chem. Phys. Lipids* 149, 28–39.

(27) Jo, E. J., McLaurin, J., Yip, C. M., St George-Hyslop, P., and Fraser, P. E. (2000) α -Synuclein membrane interactions and lipid specificity. *J. Biol. Chem.* 275, 34328–34334.

(28) Zhu, M., Li, J., and Fink, A. L. (2003) The association of α -synuclein with membranes affects bilayer structure, stability, and fibril formation. *J. Biol. Chem.* 278, 40186–40197.

(29) Sciacca, M. F., Kotler, S. A., Brender, J. R., Chen, J., Lee, D. K., and Ramamoorthy, A. (2012) Two-step mechanism of membrane disruption by A β through membrane fragmentation and pore formation. *Biophys. J.* 103, 702–710.

(30) Radovan, D., Opitz, N., and Winter, R. (2009) Fluorescence microscopy studies on islet amyloid polypeptide fibrillation at heterogeneous and cellular membrane interfaces and its inhibition by resveratrol. *FEBS Lett.* 583, 1439–1445.

(31) Weise, K., Radovan, D., Gohlke, A., Opitz, N., and Winter, R. (2010) Interaction of hIAPP with model raft membranes and pancreatic β -cells: Cytotoxicity of hIAPP oligomers. *ChemBioChem* 11, 1280–1290.

(32) Wakabayashi, M., and Matsuzaki, K. (2009) Ganglioside-induced amyloid formation by human islet amyloid polypeptide in lipid rafts. *FEBS Lett.* 583, 2854–2858.

(33) Cho, W. J., Trikha, S., and Jeremic, A. M. (2009) Cholesterol regulates assembly of human islet amyloid polypeptide on model membranes. *J. Mol. Biol.* 393, 765–775.

(34) Trikha, S., and Jeremic, A. M. (2011) Clustering and internalization of toxic amylin oligomers in pancreatic cells require plasma membrane cholesterol. *J. Biol. Chem.* 286, 36086–36097.

(35) Morita, M., Vestergaard, M., Hamada, T., and Takagi, M. (2010) Real-time observation of model membrane dynamics induced by Alzheimer's amyloid β . *Biophys. Chem.* 147, 81–86.

(36) Domanov, Y. A., and Kinnunen, P. K. J. (2008) Islet amyloid polypeptide forms rigid lipid-protein amyloid fibrils on supported phospholipid bilayers. *J. Mol. Biol.* 376, 42–54.

(37) Lundbaek, J. A., Collingwood, S. A., Ingolfsson, H. I., Kapoor, R., and Andersen, O. S. (2010) Lipid bilayer regulation of membrane protein function: Gramicidin channels as molecular force probes. *J. R. Soc., Interface* 7, 373–395.

(38) Smith, P. E. S., Brender, J. R., and Ramamoorthy, A. (2009) Induction of negative curvature as a mechanism of cell toxicity by amyloidogenic peptides: The case of islet amyloid polypeptide. *J. Am. Chem. Soc.* 131, 4470–4478.

(39) Cazzaniga, E., Bulbarelli, A., Lonati, E., Orlando, A., Re, F., Gregori, M., and Masserini, M. (2011) A β peptide toxicity is reduced after treatments decreasing phosphatidylethanolamine content in differentiated neuroblastoma cells. *Neurochem. Res.* 36, 863–869.

(40) Janmey, P. A., and Kinnunen, P. K. J. (2006) Biophysical properties of lipids and dynamic membranes. *Trends Cell Biol.* 16, 538–546.

(41) Walsh, D. M., Klyubin, I., Fadeeva, J. V., Cullen, W. K., Anwyl, R., Wolfe, M. S., Rowan, M. J., and Selkoe, D. J. (2002) Naturally secreted oligomers of amyloid β protein potently inhibit hippocampal long-term potentiation in vivo. *Nature* 416, 535–539.

(42) Lin, C. Y., Gurlo, T., Kaye, R., Butler, A. E., Haataja, L., Glabe, C. G., and Butler, P. C. (2007) Toxic human islet amyloid polypeptide (h-IAPP) oligomers are intracellular, and vaccination to induce anti-toxic oligomer antibodies does not prevent h-IAPP-induced β -cell apoptosis in h-IAPP transgenic mice. *Diabetes* 56, 1324–1332.

(43) Vance, J. E. (2008) Thematic review series: Glycerolipids. Phosphatidylserine and phosphatidylethanolamine in mammalian cells: Two metabolically related aminophospholipids. *J. Lipid Res.* 49, 1377–1387.

(44) Brender, J. R., Hartman, K., Nanga, R. P., Popovych, N., de la Salud Bea, R., Vivekanandan, S., Marsh, E. N., and Ramamoorthy, A. (2010) Role of zinc in human islet amyloid polypeptide aggregation. *J. Am. Chem. Soc.* 132, 8973–8983.

(45) Soong, R., Brender, J. R., Macdonald, P. M., and Ramamoorthy, A. (2009) Association of highly compact type II diabetes related islet amyloid polypeptide intermediate species at physiological temperature revealed by diffusion NMR spectroscopy. *J. Am. Chem. Soc.* 131, 7079–7085.

(46) Brender, J. R., Durr, U. H. N., Heyl, D., Budarapu, M. B., and Ramamoorthy, A. (2007) Membrane fragmentation by an amyloidogenic fragment of human islet amyloid polypeptide detected by solid-state NMR spectroscopy of membrane nanotubes. *Biochim. Biophys. Acta* 1768, 2026–2029.

(47) Muller, P., Schiller, S., Wieprecht, T., Dathe, M., and Herrmann, A. (2000) Continuous measurement of rapid transbilayer movement of a pyrene-labeled phospholipid analogue. *Chem. Phys. Lipids* 106, 89–99.

(48) Stewart, J. C. (1980) Colorimetric determination of phospholipids with ammonium ferrioxalate. *Anal. Biochem.* 104, 10–14.

(49) Kodaka, M. (2004) Requirements for generating sigmoidal time-course aggregation in nucleation-dependent polymerization model. *Biophys. Chem.* 107, 243–253.

(50) Magzoub, M., and Miranker, A. D. (2012) Concentration-dependent transitions govern the subcellular localization of islet amyloid polypeptide. *FASEB J.* 26, 1228–1238.

(51) Bechinger, B., and Lohner, K. (2006) Detergent-like actions of linear amphipathic cationic antimicrobial peptides. *Biochim. Biophys. Acta* 1758, 1529–1539.

(52) Reynolds, N. P., Soragni, A., Rabe, M., Verdes, D., Liverani, E., Handschin, S., Riek, R., and Seeger, S. (2011) Mechanism of membrane interaction and disruption by α -synuclein. *J. Am. Chem. Soc.* 133, 19366–19375.

(53) Jan, A., Adolfsson, O., Allaman, I., Buccarello, A. L., Magistretti, P. J., Pfeifer, A., Muhs, A., and Lashuel, H. A. (2011) A β 42 neurotoxicity is mediated by ongoing nucleated polymerization process rather than by discrete A β 42 species. *J. Biol. Chem.* 286, 8585–8596.

(54) Pellarin, R., Friedman, R., and Caffisch, A. (2009) Amyloid aggregation on lipid bilayers and its impact on membrane permeability. *J. Mol. Biol.* 387, 407–415.

(55) Michikawa, M., Gong, J. S., Fan, Q. W., Sawamura, N., and Yanagisawa, K. (2001) A novel action of Alzheimer's amyloid β -protein (A β): Oligomeric A β promotes lipid release. *J. Neurosci.* 21, 7226–7235.

(56) Kagan, B. L., and Thundimadathil, J. (2010) Amyloid peptide pores and the β sheet conformation. *Proteins* 677, 150–167.

(57) Jang, H. B., Zheng, J., Lal, R., and Nussinov, R. (2008) New structures help the modeling of toxic amyloid β ion channels. *Trends Biochem. Sci.* 33, 91–100.

(58) Apostolidou, M., Jayasinghe, S. A., and Langen, R. (2008) Structure of α -helical membrane-bound hIAPP and its implications for membrane-mediated misfolding. *J. Biol. Chem.* 283, 17205–17210.

(59) Matsuzaki, K., Sugishita, K., Ishibe, N., Ueha, M., Nakata, S., Miyajima, K., and Epand, R. M. (1998) Relationship of membrane curvature to the formation of pores by magainin 2. *Biochemistry* 37, 11856–11863.

(60) Konarkowska, B., Aitken, J. F., Kistler, J., Zhang, S. P., and Cooper, G. J. S. (2006) The aggregation potential of human amylin

determines its cytotoxicity towards islet β -cells. *FEBS J.* 273, 3614–3624.

(61) Warschawski, D. E., Fellmann, P., and Devaux, P. F. (1996) High resolution p-31-h-1 two-dimensional nuclear magnetic resonance spectra of unsonicated lipid mixtures spinning at the magic-angle. *Eur. Biophys. J. Biophys. Lett.* 25, 131–137.

(62) Lindstrom, F., Bokvist, M., Sparrman, T., and Grobner, G. (2002) Association of amyloid- β peptide with membrane surfaces monitored by solid state NMR. *Phys. Chem. Chem. Phys.* 4, 5524–5530.

(63) Butterfield, S. M., and Lashuel, H. A. (2010) Amyloidogenic protein membrane interactions: Mechanistic insight from model systems. *Angew. Chem., Int. Ed.* 49, 5628–5654.

(64) Hallock, K. J., Lee, D. K., and Ramamoorthy, A. (2003) MSI-78, an analogue of the magainin antimicrobial peptides, disrupts lipid bilayer structure via positive curvature strain. *Biophys. J.* 84, 3052–3060.

(65) Heller, W. T., He, K., Ludtke, S. J., Harroun, T. A., and Huang, H. W. (1997) Effect of changing the size of lipid headgroup on peptide insertion into membranes. *Biophys. J.* 73, 239–244.

(66) Nanga, R. P. R., Brender, J. R., Xu, J. D., Veglia, G., and Ramamoorthy, A. (2008) Structures of rat and human islet amyloid polypeptide IAPP(1–19) in micelles by NMR spectroscopy. *Biochemistry* 47, 12689–12697.

(67) Nanga, R. P. R., Brender, J. R., Vivekanandan, S., Popovych, N., and Ramamoorthy, A. (2009) NMR structure in a membrane environment reveals putative amyloidogenic regions of the SEVI precursor peptide PAP(248–286). *J. Am. Chem. Soc.* 131, 17972–17979.

(68) Brender, J. R., Hartman, K., Gottler, L. M., Cavitt, M. E., Youngstrom, D. W., and Ramamoorthy, A. (2009) Helical conformation of the SEVI precursor peptide PAP(248–286), a dramatic enhancer of HIV infectivity, promotes lipid aggregation and fusion. *Biophys. J.* 97, 2474–2483.

(69) Munch, J., Rucker, E., Standker, L., Adermann, K., Goffinet, C., Schindler, M., Wildum, S., Chinnadurai, R., Rajan, D., Specht, A., Gimenez-Gallego, G., Sanchez, P. C., Fowler, D. M., Koulov, A., Kelly, J. W., Mothes, W., Grivel, J. C., Margolis, L., Keppler, O. T., Forssmann, W. G., and Kirchhoff, F. (2007) Semen-derived amyloid fibrils drastically enhance HIV infection. *Cell* 131, 1059–1071.

(70) Nanga, R. P. R., Brender, J. R., Vivekanandan, S., and Ramamoorthy, A. (2011) Structure and membrane orientation of IAPP in its natively amidated form at physiological pH in a membrane environment. *Biochim. Biophys. Acta* 1808, 2337–2342.

(71) Jang, H., Arce, F. T., Ramachandran, S., Capone, R., Lal, R., and Nussinov, R. (2010) β -Barrel topology of Alzheimer's β -amyloid ion channels. *J. Mol. Biol.* 404, 917–934.

(72) Vaiana, S. M., Ghirlando, R., Yau, W. M., Eaton, W. A., and Hofrichter, J. (2008) Sedimentation studies on human amylin fail to detect low-molecular-weight oligomers. *Biophys. J.* 94, L45–L47.

(73) Zhang, Y. J., Shi, J. M., Bai, C. J., Wang, H., Li, H. Y., Wu, Y., and Ji, S. R. (2012) Intra-membrane oligomerization and extra-membrane oligomerization of amyloid- β peptide are competing processes as a result of distinct patterns of motif interplay. *J. Biol. Chem.* 287, 748–756.

(74) Lee, C. C., Sun, Y., and Huang, H. W. (2012) How type II diabetes-related islet amyloid polypeptide damages lipid bilayers. *Biophys. J.* 102, 1059–1068.